Optically Pumped NH₃ as a High-Gain Amplifier for CO₂ Laser Radiation

Jonathon D. White and John Reid

Abstract—Optically pumped high-pressure mixtures of NH_3 in N_2 are shown to be efficient broad-band amplifiers of pulsed CO_2 radiation. In a dilute NH_3 mixture at 6 atm a single-pass gain of 150 (21.8 dB) was measured for the 10P(34) CO_2 transition. Gain was observed in NH_3 at pressures as high as 10 atm. Experimental measurements were made for a range of wavelengths in the 10.7 μm region, and the results compared with calculations based on a rate-equation model.

I. INTRODUCTION

A good deal of research has been carried out to model and optimize the performance of NH_3 oscillators and amplifiers in the 12 μm region [1]–[3]. These oscillators and amplifiers have been shown to be highly efficient converters of 9 μm CO_2 radiation to radiation in the 10 to 14 μm region [2]–[5]. Both the oscillators and the amplifiers typically use a dilute mixture of ammonia in an argon or nitrogen buffer gas, and are generally operated at pressures below 1 atm. Some preliminary work has been carried out to characterize the behavior of NH_3 amplifiers and oscillators at pressures exceeding 1 atm [6], [7], but the performance of such systems has been far from optimum.

The chief advantage of operating optically pumped mixtures above 1 atm is the increased bandwidth available at higher pressures. At pressures of several atmospheres, the pressure broadened bandwidth allows for continuous tunability over large segments of the 800–1000 cm^{-1} region, and enables amplification or generation of short laser pulses. Currently, much of the work on generating picosecond pulses in the midinfrared has centered on the development of multiatmosphere-discharge-excited CO_2 lasers [8]. However, there are several problems associated with high pressure discharge systems. These problems include discharge instabilities (arcs), damage to incavity optics, and the requirement for very high voltages. In light of these concerns, optical pumping of high pressure CO_2 has recently been suggested as an alternative approach [9].

In this paper, we examine optical pumping as a technique for generating large gain bandwidth in the 10 μm region, but consider NH_3 as the infrared-active gas, rather

than CO_2. The NH_3 system has gain in regions overlapping the 10.6 μm CO_2 band, and, for optical pumping, the polar NH_3 molecule possesses several advantages relative to CO_2. We have developed a set of rate equations to model the NH_3 system, and have verified the model by experimental measurements at a number of frequencies, pressures, concentrations and temperatures. Experimentally, single pass gains of 150 (21.8 dB) are observed in dilute NH_3 mixtures at 6 atm for the 10P(34) CO_2 transition. At this pressure the gain bandwidth in NH_3 is ~4 cm^{-1}, suitable for amplifying pulses as short as a few picoseconds. Our measurements indicate that optically pumped NH_3 is a viable alternative to multiatmosphere CO_2 discharge amplifiers for many applications.

II. MODEL

A rate equation approach has been used successfully to model the behavior of NH_3 systems operating at pressures below one atmosphere [1], [5]. The rate equation approach involves balancing the rate of molecules pumped up from the ground state to the $\nu_2 = 1$ level of NH_3 with the rate of molecules decaying via collisional relaxation and stimulated emission. The rate equation approach is illustrated in Fig. 1. The NH_3 energy levels can be represented by a series of anharmonic vibrational levels, upon which rotational levels are superimposed. In an exact treatment, each of these vibrational-rotational levels must be handled individually. However, for dilute mixtures (low concentrations) of NH_3, fast rotational relaxation rates ensure that only small perturbations from the thermal rotational distribution can occur within a given vibrational level. Thus, we have chosen to develop a simple model which assumes that the rotational populations within a vibrational level are always in thermal equilibrium [10]. Optical pumping by the $9R(30)$ CO_2 transition transfers population to the $\nu_2 = 1$ vibrational level. The relaxation of this population back to the ground state is dominated by vibrational-translational (VT, R) relaxation processes. The model calculates the instantaneous population in the $\nu_2 = 1$ vibrational level, and uses this population to calculate the gain on individual rotational-vibrational transitions between the ground state and the $\nu_2 = 1$ vibrational level. To account for high pressure operation, the model considers each transition to have the appropriate pressure-broadened Lorentz line shape, and sums the contributions from overlapping lines. The pos-
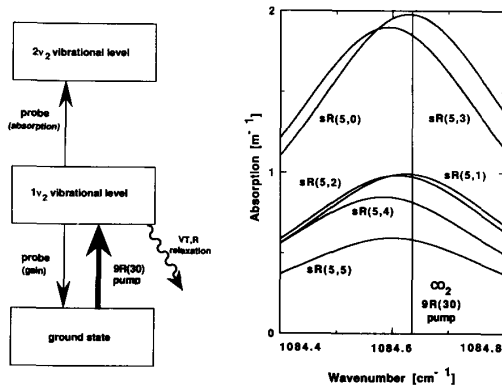
Fig. 1. Illustration of the relevant vibrational energy levels and spectroscopy of the NH_3 laser. The CO_2 $9R(30)$ pump transfers population from the ground state to the $1\nu_2$ vibrational level. Relaxation back to the ground state is dominated by VT, R collisions. The probe radiation interacts with transitions in both the $(1\nu_2 \leftarrow gs)$ and $(2\nu_2 \leftarrow 1\nu_2)$ bands. Also shown are calculated spectra for the individual pressure-broadened transitions in the $sR(5,K)$ multiplet. The spectra were calculated for a concentration of 0.1% NH_3 in 2 atm of N_2 at 200 K. The line at 1084.635 cm^{-1} indicates the position of the $9R(30)$ CO_2 pump transition.

sibility of absorption due to transitions from the $\nu_2 = 1$ to $\nu_2 = 2$ vibrational levels must also be considered [7]. These hot-band transitions overlap the region of gain for the $\nu_2 = 1$ band, and hot-band absorption reduces or eliminates gain at many wavelengths. The model calculates this absorption and subtracts it from the gain calculated for the ground state to $\nu_2 = 1$ transitions.

For each of the two vibrational bands included in the model, the ortho and para species of NH_3 [11] are treated separately. The collisional transfer of energy between the two species is slow [12], and is ignored in the present model. However, at high pressure the $9R(30)$ CO_2 radiation pumps transitions in both ortho and para NH_3. As can be seen in Fig. 1, the *total* absorption of the pump radiation by ortho and para transition is approximately equal, and, as a consequence, each species produces a similar level of inversion [13]. The total pump absorption and probe amplification is calculated by summing the contributions from ortho and para species in the $(1\nu_2 \leftarrow gs)$ and $(2\nu_2 \leftarrow 1\nu_2)$ bands.

The equations given below are the rate equations which are used to calculate the population in the three vibrational levels shown in Fig. 1. These equations are applied separately to ortho- and para-NH_3.

$$\frac{dN_0}{dt} = -\frac{dN_1}{dt} = \frac{N_1 - A \times N_0}{\tau_{VT}} - P. \qquad (1)$$

N_0 and N_1 represent the populations in the ground state and $\nu_2 = 1$ level. The population of the $\nu_2 = 2$ level, N_2, is considered to remain in thermal equilibrium with the $\nu_2 = 1$ level [14], and it is assumed that $N_0 + N_1 + N_2 = N$, the total population (i.e., only the three levels shown in Fig. 1 contain significant population). In (1), A is the thermal equilibrium ratio of N_1/N_0 and τ_{VT} is the VT, R relaxation rate from the $\nu_2 = 1$ vibrational level to the

ground state. The pumping term P is the rate of optical pumping of molecules into the first vibrational level from the ground state. This rate is the sum of the pumping on the individual transitions. In the case of ortho-NH_3, the overall rate involves summing the overlapping absorptions from the $sR(5,0)$ and $sR(5,3)$ transitions. The individual pumping rates are given by:

$$P_i = \frac{I_p(t)}{h\nu_p} \times \alpha \ (\nu_p). \qquad (2)$$

$I_p(t)$ is the intensity of the pump pulse, $h\nu_p$ is the energy per photon at the pump frequency (ν_p), and α is the absorption at the pump frequency for a given transition. The absorption is given by:

$$\alpha(\nu) = \sigma(\nu) \times \left(f_l \times N_0 - f_u \times N_1 \times \frac{g_l}{g_u} \right) \qquad (3)$$

where $\sigma(\nu)$ is the absorption cross section for the transition at frequency ν, f_l and f_u are the fraction of molecules in the lower and upper rotational levels of the pumped transition, while g_l and g_u are their respective degeneracies.

Equations (1)–(3) are solved numerically for N_1/N_0 as a function of time. The calculated values of N_1/N_0 are then used to determine the gain on the individual transitions. In addition, a knowledge of the ratio N_1/N_0 allows one to calculate the hot-band absorptions since the $2\nu_2$ vibrational level can be assumed to be in thermal equilibrium with the $1\nu_2$ vibrational level (i.e., at 200 K, $N_2 = 0.0062$ N_1 [15]). The contributions from all transitions are then summed to give the total overlapping gain or absorption at the pump and probe frequencies. This sum is carried out by assuming that all rotational-vibrational transitions have the same pressure broadening coefficient. This assumption is based on the work of Beckwith *et al.* [16] who measured the relevant pressure-broadening coefficients on a number of NH_3 transitions and determined that the values agreed within $\pm 20\%$. Table I lists the molecular constants used in the model.

As the pump beam propagates down the amplifier cell, its intensity decreases due to absorption. This depletion in pump intensity is given by:

$$\frac{dI_p(x, t)}{dx} = \alpha(x, t, \nu_p) \times I_p(x, t) \qquad (4)$$

where $\alpha(x, t, \nu_p)$ is the absorption of the pump radiation due to all NH_3 transitions. To evaluate the total gain in the cell this attenuation of the pump is taken into account by splitting the gain cell into small sections and calculating the gain and pump absorption for each section.

Fig. 2 shows the results obtained by calculating gain for a short NH_3 cell pumped at 25 MW/cm^2—a typical experimental pump intensity. In the 800 to 1000 cm^{-1} region there are significant areas of both gain and absorption. The absorbing regions are a result of the transitions from the $1\nu_2$ to $2\nu_2$ level. Fig. 2 clearly demonstrates the

TABLE I
PHYSICAL CONSTANTS USED IN THE MODELING OF HIGH PRESSURE ^{14}NH₃ AMPLIFIERS

Collision Partner	VT, R Relaxation rates [μs^{-1} torr^{-1}] Temperature	
	200 K	300 K
NH₃	1.14 [a]	1.45 [a]
Ar	0.0035 [b]	0.0059 [c]
N₂	0.0075 [a]	0.0102 [a]

Buffer gas	Pressure broadening coefficients [MHz/torr] Temperature	
	200 K	300 K
Ar	4.9 [d]	3.5 [e]
N₂	2.0 [d]	1.5 [e]

Dipole moments for ν_2 band [D]	
$1a \leftarrow 0s$	0.237 [e]
$1s \leftarrow 0a$	0.244 [e]
$2a \leftarrow 1s$	0.28 [f]
$2s \leftarrow 1a$	0.42 [f]

[a]Danagher and Reid [12]
[b]Hovis and Moore [17]
[c]Hovis and Moore [18]
[d]pressure broadening at 200 K is estimated from the broadening coefficients at 300 K using the relationship given by Townes and Schawlow [19]:

$$\Delta \nu \propto T^{-(n+1)/2(n-1)}$$

where T is the temperature and $n = 7$ for Ar-NH₃ collisions and $n = 4$ for N₂-NH₃ collisions.
[e]Beckwith, Danagher and Reid [16]
[f]Dubé and Reid [14]
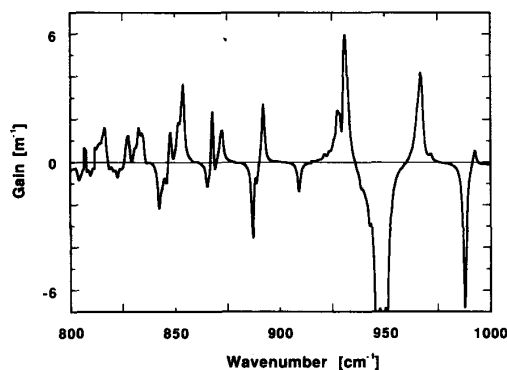
Fig. 2. Calculated gain and absorption in NH₃ for a peak pump intensity of 25 MW/cm². The calculation is carried out for a 0.12% NH₃ in N₂ mixture at 6.33 atm and 200 K.

importance of including hot-band transitions in the model. Any model which calculates gain based solely on the regular band transitions will greatly overestimate the extent of gain in a high-pressure system. (The importance of the overlying hot band was first pointed out by Morrison et al. [7].) From Fig. 2, it is clear that the model calculations predict maximum gain in the region from 926 to 938 cm^{-1} while the region of strongest absorption is from 938 to 955 cm^{-1}. This strong absorption is caused by the overlapping sQ-branch transitions of the hot band, while the gain at 932 cm^{-1} is due to the overlapping aQ-branch transitions of the regular band. The fact that the regions
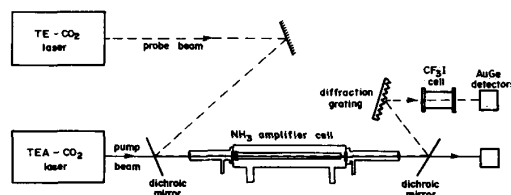
Fig. 3. Schematic diagram of the apparatus for measuring gain in high-pressure NH₃ mixtures. The high-pressure NH₃ amplifier is comprised of a pyrex waveguide surrounded by an aluminum cylinder. It is designed with pyrex extension tubes to ensure that the cold salt windows do not come into contact with the moist room air. In addition the pyrex extension at the input acts as a spatial filter to eliminate hot spots in the pump beam.
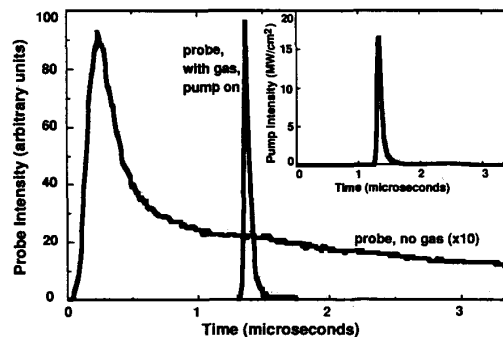
Fig. 4. Typical probe and pump pulses used in the experiment. The inset shows the 9R(30) pump pulse, while the main traces show the 10P(34) probe pulse, both with and without amplification in a 0.1% NH₃ in N₂ mixture at 5.3 atm and 200 K. At the peak of the pump pulse, the probe is amplified by a factor of 45. The cell length is 88 cm.

of maximum gain and absorption are associated with the Q-branch transitions is very significant from a modeling point of view, as Morrison et al. [1] have shown that the exact value of gain or absorption in the Q-branch is extremely sensitive to the value of N_1/N_0.

Thus, the wavelength region from 926 to 955 cm^{-1} provide both the largest experimental signals, and the most sensitive test of the model predictions. We have therefore chosen this wavelength region for our experiments, and in the next section, we describe the experimental apparatus for making small-signal gain measurements in the 926 to 955 cm^{-1} region.

III. EXPERIMENTAL SETUP

Fig. 3 is a schematic of the experimental apparatus. An atmospheric-pressure TE-CO₂ laser operating on the 9R(30) transition was used to pump a high-pressure NH₃ cell. The gas mixture in the pump laser was adjusted to provide a 100 ns FWHM pulse with minimal tail. For the probe laser, a second TE-CO₂ laser operating at 400 torr provided a relatively long pulse, as shown in Fig. 4. Thus, under the typical experimental conditions, the pump-induced gain or absorption can be measured from a single trace. By line-tuning the probe laser from 10P(8) to 10P(38), the wavelength region of interest can easily be covered. The NH₃ cell (Fig. 3) typically contained a mix-

ture of $<0.1\%$ NH_3 in a buffer gas. A dichroic mirror and grating were used to separate the probe and pump pulse. A gas cell filled with CF_3I was placed before the probe detector to absorb residual 9 μm radiation. Both the pump and probe pulses were detected using Au : Ge detectors. The signals from the detectors were recorded by a fast digital oscilloscope (10 ns per point). Fifty successive pulses were averaged, and the resultant trace transferred to a computer for analysis.

IV. RESULTS

Fig. 5 is an example of the type of measurement taken in comparing calculations and experiment. The $10P(36)$ CO_2 pulse probes an area of the spectrum dominated by $1\nu_2 \leftarrow gs$ transitions. Thus, in the absence of the $9R(30)$ pump the probe experiences absorption. However, with the $9R(30)$ pump traveling collinearly, the population is inverted and a gain spike appears on the $10P(36)$ CO_2 pulse. As the collisional relaxation time is 22 ns, the gain quickly decays after the pump pulse. Model calculations agree closely with experimental measurements at the peak and exhibit reasonable agreement in the tail of the pump pulse.

As it is relatively simple to grating-tune the CO_2 probe laser, measurements were also made on the CO_2 lines surrounding $10P(36)$. Fig. 6 summarizes the results of these measurements and compares them with calculations. The lower trace compares the absorption measured by passing *only* the probe through the amplifier with that calculated from the model. The good agreement between calculations and experiment serves as a check on both the pressure-broadening coefficients and the experimental NH_3 concentration. The concentration is determined using calibrated flowmeters. The upper trace in Fig. 6 demonstrates the excellent agreement between experiment and theory at the peak of the pump pulse. The experimental NH_3 concentration was chosen so that both gain and absorption could be measured at the same time. Thus on $10P(34)$, we were able to observe an absorption of $6\%/cm$ change into a gain of $2\%/cm$ when the $9R(30)$ pump pulse was present. Moving across the profile, gain is seen to vary from $1\%/cm$ on those transitions with the strongest absorptions to zero on those with weak absorptions in accord with calculations. The bandwidth of the gain is ~ 4 cm^{-1}. This bandwidth is sufficient to amplify a CO_2 laser pulse as short as a few picoseconds.

As seen in Fig. 2, in addition to predicting regions of strong gain, the model also predicts regions of strong absorption, particularly around 950 cm^{-1}. This region was probed using the $10P(14)$ CO_2 transition and the results are shown in Fig. 7. In contrast to the gain seen on $10P(36)$, $10P(14)$ experiences greatly increased absorption in the presence of the pump pulse. This increased absorption is evident well into the tail of the pump pulse and is quite sensitive to the actual value of the pump intensity (The second drop in transmission is due to an increase in intensity in the tail of the $9R(30)$ pump pulse).
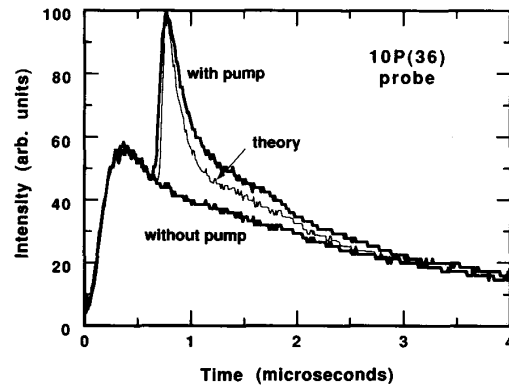
Fig. 5. Comparison between theory and experiment for the amplification of a $10P(36)$ CO_2 probe pulse. The NH_3 concentration is 0.007% NH_3 in 8.33 atm of N_2 at 200 K. The peak pump intensity is 8.4 MW/cm^2 at the input to the 88 cm cell.
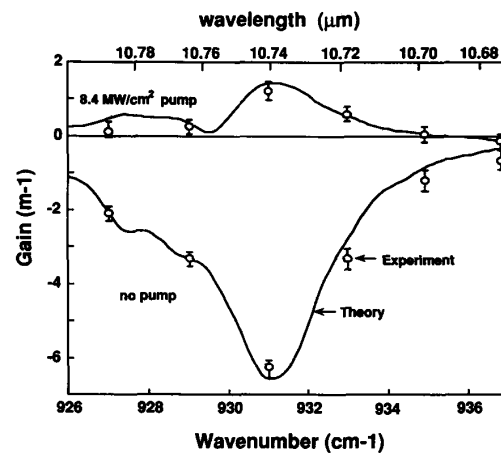
Fig. 6. Comparison of theory and experiment for measurements made at six different CO_2 probe transitions. The theoretical lines are calculated for a mixture of 0.04% NH_3 in 5.5 atm of N_2 at 200 K, pumped with a peak intensity of 8.4 MW/cm^2. The measured points are obtained with and without the pump beam in the cell.
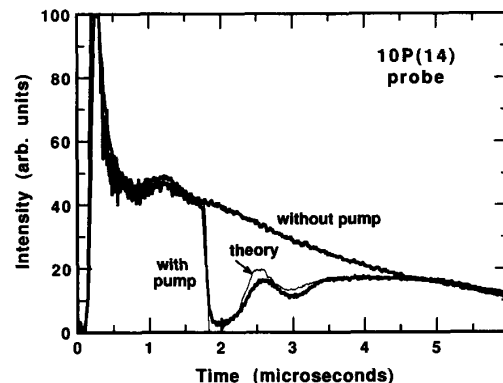
Fig. 7. Comparison between theory and experiment for the attenuation of a $10P(14)$ CO_2 probe pulse. The concentration is 0.07% NH_3 in 5.33 atm of N_2 at 200 K. The peak pump intensity is 8.4 $MW/cm2$ at the input to the 88 cm cell.
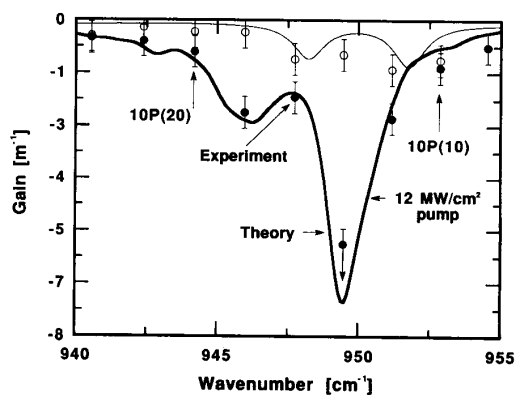
Fig. 8. Comparison of theory and experiment for measurements made between 940 and 955 cm^{-1}. The theoretical lines are calculated for a concentration of 0.04% NH_3 in 5.3 atm of N_2 at 200 K. The upper trace represents absorption with the pump absent, and the lower trace shows the absorption at the peak of the 12 MW/cm^2 $9R(30)$ pump pulse. The experimental points are determined by scanning the CO_2 probe laser from $10P(22)$ to $10P(8)$.

Tuning the probe laser around the $10P(14)$ transitions enabled us to trace out the pump-induced absorption profile in this region. The results of these measurements are compared with model calculations in Fig. 8. In contrast to Fig. 6, the upper trace represents the absorption with the pump absent. The lower trace indicates the absorption at the peak of the pump pulse. Here, as in Fig. 6, the main sources of experimental error are due to fluctuations in concentration, pulse to pulse variations in the pump pulse shape, and digitalization inaccuracies. In the case of $10P(14)$, the pump induced absorption was so strong that there was minimal transmission of the probe—hence the larger error bounds. Once again reasonable agreement is seen between experiment and theory at the peak of the pulses for this region dominated by $2\nu_2 \leftarrow 1\nu_2$ absorptions.

V. DISCUSSION AND CONCLUSIONS

The results shown in Figs. 4 to 8 demonstrate that good agreement exists between calculations and measurements at the peak of the $9R(30)$ pump pulse for CO_2 probe frequencies varying from 925–955 cm^{-1} ($10P(8)$ to $10P(38)$). Reasonable temporal agreement is also seen for the two CO_2 probe transitions illustrated in Figs. 5 and 7. Similar agreement between theory and experiment was found over a wide range of concentrations (0.01–0.1% NH_3), pressure (1–10 atm), temperature (200 and 300 K) and for both argon and nitrogen buffer gases. These results confirm that the rate equation model can predict the operation of the high pressure NH_3 amplifier over a wide range of conditions.

The experimental measurements shown in Figs. 5 to 8 were all made at dry ice temperatures. The amplifier was cooled to 200 K because theory predicts, and experiment confirmed, that significantly better performance is obtained at this temperature than at room temperature. This increased performance is due to the larger pressure broad-

ening coefficient, slower VT, R relaxation rates, and more favorable partition function at lower temperatures. For example, to achieve a 4 cm^{-1} bandwidth with a 2.8%/cm gain requires a 9 MW/cm^2 pump at 200 K and a 29 MW/cm^2 pump at 300 K. The inferior amplifier performance at 300 K demonstrates that a high pressure NH_3 amplifier should be operated at 200 K. [Little benefit is obtained by lowering the temperature much below 200 K, as the NH_3 begins to freeze out at 175 K.]

Having verified the model it is interesting to examine the behavior of the amplifier under more extreme conditions. Experimentally, with increased concentration (0.12% NH_3) and pump intensity (25 MW/cm^2), single pass gains of 150 (5.7 m^{-1}) were observed at 6.33 atm in agreement with the predictions of the model. This performance is comparable to the best obtainable in CO_2 discharge modules without the problems associated with high pressure electrical discharges.

With the present apparatus, the CO_2 laser output power limits us to a peak pump intensity of ~25 MW/cm^2 (~3 J/cm^2 for the pulses shown in Fig. 3). If we increase the flux density to 5 J/cm^2 for the pulses shown in Fig. 3, we should be able to pump with peak intensities of 40 MW/cm^2. The model predicts single pass gains in excess of 60 dB at 6 atm are achievable under these pumping conditions—significantly better performance than that attainable with high-pressure CO_2 discharges. A further improvement in NH_3 amplifier performance can be obtained by pumping with shorter CO_2 pump pulses. Preliminary model calculations indicate that a 3 J/cm^2 pump pulse with a FWHM of 10 ns incident upon an optimized NH_3 amplifier will produce a single pass gain of 61 dB on the $10P(34)$ CO_2 transition at a pressure of 20 atm.

These results and calculations show clearly that optically pumped NH_3 is a viable alternative to discharge-excited CO_2 as high-pressure amplifier for CO_2 radiation, offering both high-gain and large bandwidth.

REFERENCES

[1] H. D. Morrison, B. K. Garside, and J. Reid, "Dynamics of the optically pumped midinfrared NH₃ laser at high pump power—Part I: Inversion gain," *IEEE J. Quantum Electron.*, vol. QE-20, pp. 1051–1060, 1984.

[2] B. I. Vasil'ev, A. Z. Grasyuk, A. P. Dyad'kin, A. N. Sukhanov, and A. B. Yastrebkov, "High-power efficient optically pumped NH₃ laser, tunable over the range 770–890 cm−1," *Sov. J. Quantum Electron.*, vol. 10, pp. 64–68, 1983.

[3] P. K. Gupta, A. K. Kar, M. R. Taghizadeh, and R. G. Harrison, "12.8-μm NH₃ laser with emission with 40–60% power conversion and up to 28% energy conversion efficiency," *Appl. Phys. Lett.*, vol. 39, pp. 32–34, 1981.

[4] D. M. Bruce, A. Chakrabarti, J. Reid, and J. D. White, "Efficient, optically-pumped NH₃ oscillators and amplifiers operating in the mid-infrared," presented at the CLEO Conf., Anaheim, CA, 1988, paper THT1.

[5] J. D. White, D. M. Bruce, P. H. Beckwith, and J. Reid, "Efficient optically pumped NH₃ amplifiers in the 10 to 12 μm region," *Appl. Phys. B*, vol. 50, pp. 345–354, 1990.

[6] M. Akhrarov, B. I. Vasil'ev, A. Z. Grasyuk, and V. I. Soskov, "Ammonia laser pumped transversely by optical radiation," *Sov. J. Quantum Electron.*, vol. 16, pp. 453–455, 1986.

[7] H. D. Morrison, B. K. Garside, and J. Reid, "Modeling of high-pressure 12-μm NH₃ lasers," *Appl. Phys. B*, vol. 37, pp. 165–170, 1985.

[8] P. B. Corkum, "Amplification of picosecond 10 μm pulses in multiatmosphere CO_2 lasers," *IEEE J. Quantum Electron.*, vol. QE-21, pp. 216–232, 1985.

[9] K. Stenersen and G. Wang, "New direct optical pump schemes for multiatmosphere CO_2 and N_2O lasers," *IEEE J. Quantum Electron.*, vol. 25, pp. 147–153, 1989.

[10] Detailed calculations which separate out the directly pumped levels from the rotational "bath" [5] indicate that, under the experimental conditions used in this paper, any population deviations are < 10% of the thermal equilibrium value.

[11] In ortho-NH_3, the quantum number of the component of angular momentum along the molecular axis K is equal to $3n$ [where n is zero or a positive integer], while for para-NH_3 $K = 3n + 1$. Thus $sR(5, 0)$ and $sR(5, 3)$ are ortho-transitions, while $sR(5, 1)$, $sR(5, 2)$, $sR(5, 4)$, and $sR(5, 5)$ are paratransitions.

[12] A. D. J. Danagher and J. Reid, "Vibrational relaxation of the $\nu_2 = 1$ level of ortho and para NH_3," *J. Chem. Phys.*, vol: 86, pp. 5449–5455, 1987.

[13] A very different behavior is observed when pumping low pressure NH_3 mixtures. With the $9R(30)$ CO_2 pump, only ortho NH_3 is inverted. An alternative pump wavelength must be used to invert the para species [D. F. Kroeker and J. Reid, "Line-tunable cw ortho- and para-NH_3 lasers operating at wavelengths of 11 to 14 μm," *Appl. Opt.*, vol. 25, pp. 2929–2933, 1986.]

[14] P. Dube and J. Reid, "Vibrational relaxation of the $2\nu_2$ level of NH_3," *J. Chem. Phys.*, vol. 90, pp. 2892–2899, 1989.

[15] P. Dube, *Collisional Energy Transfer From the $2\nu_2$ Level of NH_3 Measured With a Tunable Diode Laser*, Masters Thesis, McMaster University, 1988.

[16] P. H. Beckwith, D. J. Danagher, and J. Reid, "Linewidths and linestrengths in the ν_2 band of NH_3 as measured with a tunable diode laser," *J. Mol. Spec.*, vol. 121, pp. 209–217, 1987.

[17] F. E. Hovis and C. B. Moore, "Temperature dependence of vibrational energy transfer in NH_3 and $H_2^{18}O$," *J. Chem. Phys.*, vol. 72, pp. 2397–2402, 1980.

[18] F. E. Hovis and C. B. Moore, "Vibrational relaxation of $NH_3(\nu_2)$," *J. Chem. Phys.*, vol. 69, pp. 4947–4950, 1978.

[19] C. H. Townes and A. L. Schawlow, *Microwave Spectroscopy.* New York: Dover, 1975, p. 369.

Jonathon D. White, photograph and biography not available at the time of publication.

John Reid was born in Rochdale, England, on December 14, 1948. He received the B.A. degree in physics from Oxford University, Oxford, England, in 1970, and the M.Sc. and Ph.D. degrees from McMaster University, Hamilton, Ont., Canada, in 1972 and 1975, respectively.

From 1975 to 1976 he was a Research Associate at the Herzberg Institute of Astrophysics, Ottawa, Ont., Canada, where he worked on spin-flip Raman lasers and sequence CO_2 lasers. He was a faculty member of the Department of Engineering Physics, McMaster University, from 1976 to 1987, where he continued his work on infrared lasers. He developed a 4.3 μm CO_2 laser and the first CW 12 μm laser in NH_3. His research interests included trace gas detection using tunable diode lasers, and isotope separation by multiphoton dissociation. In 1988, he joined the Research and Development Department of Lumonics, Inc., where he is presently working on the development of excimer lasers.

Dr. Reid is a member of the Optical Society of America and the Canadian Association of Physicists.